Biochimica et Biophysica Acta, 1110 (1992) 97–104

BBAMEM 75751

Kinetics of melittin induced pore formation in the membrane of lipid vesicles

Gerhard Schwarz, Rui-ting Zong and Teodor Popescu

Department of Biophysical Chemistry, Biocenter of the University of Basel, Basel (Switzerland)

(Received 5 March 1992)

Key words: Channel gating; Carboxyfluorescein release; Peptide–lipid interaction

We have investigated the permeabilization of POPC unilamellar vesicle bilayers upon the addition of melittin. This process was measured in an early time range of a few minutes by means of monitoring the release of an entrapped marker, the self-quenching fluorescent dye carboxyfluorescein. Pore formation is indicated by an apparent 'all-or-none' efflux out of individual vesicles and a higher than linear dependence on melittin concentration. Applying a recently developed evaluation procedure, the data are readily converted into the gross number of pores per vesicle formed within the elapsed measuring time t. The results can be generally described in terms of a fast initial rate of pore formation that slows down to a much lower value after a period of about 1 to 2 minutes, following a single exponential time course. The three rate parameters involved are shown to be power functions of the concentration of melittin that is actually associated with the vesicle membrane. These findings are in excellent quantitiative agreement with a proposed scheme of reaction steps where the formation of lipid associated peptide dimers becomes rate determining once an initial fast deposit is exhausted.

Introduction

Melittin, the main constituent of bee venom, is an amphipathic peptide of 26 amino acid residues [1]. It has aroused considerable interest because of its actions on membranes as recently reviewed [2]. In particular, voltage-dependent pore formation in planar lipid bilayers, reflected by non-ohmic electric conductance effects, had been shown to occur below micromolar peptide concentrations [3–8]. The underlying molecular mechanism is so far unknown. Possible elucidation of the physico-chemical features of reaction steps involved in the over-all process are considered to be of fundamental significance regarding peptide (protein) incorporation and translocation in biological membranes.

In a previous publication from this laboratory some results of pertinent conductance experiments have been reported that concern planar bilayers made of pure dioleoylphosphatidylcholine (DOPC), an electrically neutral (i.e., zwitterionic) phospholipid species [9]. The observed pores exhibited a most simple opening kinetics in contrast to the somewhat complex time course of activation and inactivation phases in the case of asolectin bilayers (a mixture of charged and uncharged lipid) [4].

In addition to voltage-gated pore formation in planar lipid bilayers melittin has been shown to induce hemolysis of erythrocyte membranes. De Grado et al. [10] find that surface bound peptide produces transient openings through which hemoglobin molecules can escape following a biphasic time course. Tosteson et al. [11] have basically confirmed this phenomenon under somewhat different salt and temperature conditions but in contrast to the former work observe an 'all-or-none' lysis of the cells. They propose a colloid osmotic mechanism where the release of hemoglobin is secondary to the formation of relatively small ion permeable lesions in the membrane. In a more recent paper Portlock et al. [12] compare hemolysis with the melittin induced leakage of an internal marker from large lipid vesicles. These authors argue that the underlying mechanism in the erythrocyte membrane apparently involves the integral protein components and accordingly becomes much more complex than the one occurring in a pure lipid bilayer. In fact, this notion is supported by substantial disparities between the respective responses to various additional agents.

Under such circumstances a quantitative analysis of the effects observed with a quite simple liposome system appears to be most useful. In the present article we describe and discuss the melittin induced pore

Correspondence to: G. Schwarz, Biocenter of the University, Klingelbergstrasse 70, CH-4056 Basel, Switzerland.

formation kinetics in small unilamellar vesicle membranes of a phosphatidylcholine similar to DOPC. Our experimental approach takes advantage of pore-mediated release of carboxyfluorescein as monitored by the fluorescence signal arising from the relief of self-quenching [13]. The recorded data can be quantitatively evaluated in terms of the rate law applicable to the forward reaction of pore formation [14]. This is analysed in the light of results which we have recently obtained with regard to the basic thermodynamics and kinetics of the association of melittin with DOPC or other phosphatidylcholine vesicles [15,16]. Taken together we establish a definite relationship between the pore formation rate and the concentration of melittin that is actually associated with the vesicles. It reveals an interesting new insight into the molecular events underlying the membrane modifying action of melittin.

Materials and Methods

Melittin (research grade) was purchased from Serva Feinbiochemica (Heidelberg, Germany). Melittin stock solutions were made in 1 mg/ml of aqueous solution, the concentration being determined by UV spectroscopy using an absorption coefficient of 5570 $M^{-1}cm^{-1}$ at 280 nm [17]. An appropriate small volume of stock was diluted to prepare a fresh peptide solution for each experiment. There was no apparent effect of possible phospholipase contamination. Neither purification by pressure filtration using Diaflo YM 10 membranes [15] nor adding 1 mM EDTA to inactivate the enzyme [18] resulted in significant changes of the measured data.

The fluorescent dye 5,6-carboxyfluorescein (CF) (M_r = 376, 99% pure by HPLC) was a product of Sigma (St. Louis, MO). In order to dissolve the substance in aqueous solution and to set a pH of 7.4 its two acidic groups have been neutralized by adding the stoichiometric amount of 1 M NaOH.

Palmitoyloleoylphosphatidylcholine (POPC) as obtained from Avanti Polar Lipids (Birmingham, AL, USA) was used without further purification. Small unilamellar vesicles (SUV) were made by ultrasonic irradiation [19]. We carried out 30 min sonification of a 1 ml lipid dispersion (10 mg POPC, 10 mM Tris buffer, 100 mM NaCl, 46 mM CF (pH 7.4)) at 10°C under N_2 flow, followed by 10 min centrifugation to remove titanium. The resulting solution was passed over a Sephadex G-50 column (Pharmacia, Upsala, Sweden) with our standard buffer solution (10 mM Tris, 100 mM NaCl (pH 7.4)) in order to separate the loaded vesicles from untrapped dye. The lipid concentration of the final stock solution was determined by phosphate analysis [20,21]. The size of vesicles can be characterized by the volume of their internal aqueous compartments [22]. The final overall concentration of dye, c_∞, is determined from a fluorescence emission calibration curve after having broken up the liposomes by adding detergent and set in relation to the originally entrapped concentration, c_0. This leads to an internal trapped volume per mol lipid: $\bar{V}_i = (c_\infty/c_0)/c_L$ under the condition of a given lipid concentration c_L.

Fluorescence emission of CF was recorded at 520 nm (excitation at 490 nm) with a Series 8000 spectrofluorometer (SLM Instruments, Urbana-Champaign, IL) equipped for individual sample cell stirring and temperature control. In a typical marker release experiment we started with a 2 ml peptide solution (standard buffer, 20°C) in a stirred fluorescence cuvette. Each run was initiated by adding a certain small volume (in the range of 5–80 μl) of vesicle stock solution (it is not advisable to do it the other way around because of artefacts caused by transient spots of highly concentrated peptide [14]). Then we followed continuously the fluorescence signal F as it increased in the course of time (see inset of Fig. 1). The starting signal F_0 (at time $t = 0$ where no marker is yet released) was measured in a blank experiment without melittin. The final signal F_∞ (all dye released at $t \to \infty$) has been determined after the addition of 50 μl of a 10% Triton X-100 solution (so that the vesicles are decomposed by the detergent) and having corrected for the dilution effect.

We have measured the quenching factor $Q = F_0/F_\infty$ under the condition of carefully removed external dye and no added melittin. This resulted in $Q = 0.12(\pm 0.01)$ for $c_0 = 50$ mM CF ($Q = 0.13$ for 46 mM CF) in excellent agreement with earlier reports in the literature [23]. These experiments were repeated with vesicle solutions after about 50% efflux of entrapped dye was eventually attained owing to the action of added melittin. Once the released dye had been removed the quenching factor proved to be practically the same as measured before the addition of melittin indicating that melittin-induced dye release of individual vesicles is an 'all-or-none' event [23]. In other words, vesicles are either fully depleted of the marker or have nothing of it lost at all. This clearly suggests formation of pores instead of a permeability increase of the whole bilayer.

Theoretical basis

The formation of a pore P in a membrane by an agent A added to the external aqueous medium naturally involves at least two fundamental steps. These are (I) association of A with the lipid bilayer and (II) conversion of lipid associated A into a pore. The appropriate kinetic scheme may be formulated as

$$\text{(I) } A_{1f} + L \rightleftharpoons A_1, \qquad \text{(II) } mA_1 \rightarrow P \tag{1}$$

where A_{1f}, A_1 stand for aqueous (i.e., free) and lipid-associated monomeric A, respectively, and L is the lipid. This assumes that a pore is composed of m (≥ 1) A-monomers. The first stage actually describes the partitioning of single A-molecules between the lipid and aqueous phases.

A detailed discussion of the partitioning with regard to monomeric melittin can be found elsewhere [15]. We note that r_1, i.e., the associated monomeric peptide to lipid ratio (mol per mol), can generally be related to the free (aqueous) concentration of monomeric peptide, c_1, by the equation

$$r_1 = (\Gamma_1/\alpha_1)\cdot c_1 \tag{2}$$

with a (concentration-independent) partition coefficient Γ_1 and a pertinent thermodynamic activity coefficient α_1 taking into account the possible interaction between associated melittin molecules (mainly due to electrostatic repulsion of the inherent positive charges). Under our present conditions appreciable aggregation can be ruled out in both environements (see Discussion). Then we have

$$\ln \alpha_1 = 2\nu_c\cdot\sinh^{-1}(\nu_c\cdot b\cdot r_1) \tag{3}$$

(ν_c, effective charge number; b, a dimensionless parameter determined by the ionic strength in the aqueous medium) as derived from a Gouy-Chapman model approach [15]. Eqn. 2 may be used to express r_1 in terms of the over-all concentrations of melittin and lipid, c_M and c_L, respectively. We find that

$$r_1 = \Gamma_1\cdot c_M/(\alpha_1 + \Gamma_1\cdot c_L) \tag{4}$$

when mass conservation is taken into account.

From a kinetic point of view naturally the question arises how fast the partitioning equilibrium will be established after having mixed the peptide and vesicle solutions. In the ideal case of sufficiently low r_1 (so that $\alpha_1 = 1$) a single-exponential relaxation process can be expected with a relaxation time τ according to the relation

$$1/\tau = k_{as}\cdot c_L + k_{dis} \tag{5}$$

where k_{as} stands for the second-order rate constant of $A_{1f} + L \rightarrow A_1$ and k_{dis} denotes the first-order rate constant of the reverse reaction. Experimental data with DOPC have resulted in $k_{as} \approx 10^5\ M^{-1}s^{-1}$ and $k_{dis} \approx 10\ s^{-1}$ [15]. These orders of magnitude appear to be applicable to our POPC system as well. Therefore equilibration of the partitioning is very likely reached in a time definitely much below one second. This should even hold true if there is some slowing down effect due to electrostatic repulsion (reflected by slightly lifted values of α_1).

Turning to the second stage in the kinetic scheme 1 the rate of $m\ A_1 \rightarrow P$ may be defined as $r_p = \nu dr_p/dt$ (r_p, molar ratio of pores per lipid; ν, number of lipid molecules per vesicle). The average number of pores per vesicle, p, opened sometime between $t = 0$ and a measuring time $t > 0$ will then be obtained as

$$p(t) = \int_0^t r_p\cdot dt \tag{6}$$

This function $p(t)$ can be determined directly from the experimental release data expressed in terms of a normalized efflux function

$$E(t) = (F_\infty - F)/(F_\infty - F_0) \tag{7a}$$

It has been shown that

$$p(t) = -\ln E(t) \tag{7b}$$

provided one deals with an 'all-or-none' case of release where a vesicle is fully depleted through the first pore being formed [14]. This basic condition has indeed been experimentally confirmed for the present system as pointed out above. Thus the values of $E(t)$ recorded in the release experiments are readily converted to a plot of p versus time. The slope of this curve will then be equal to r_p.

Results

The present experiments primarily focus on the pore formation rate under the condition of varying the

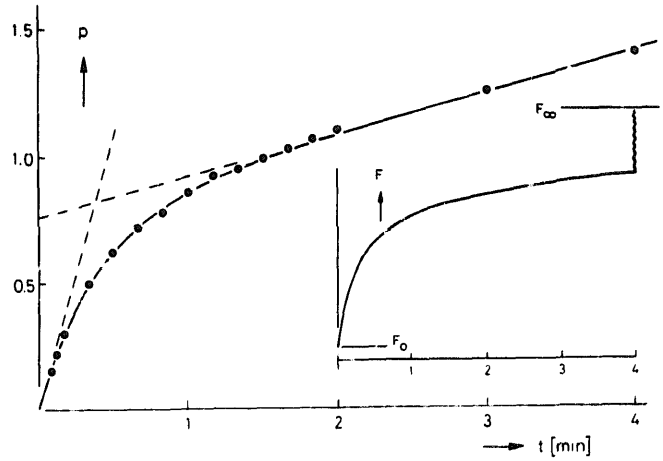

Fig. 1. A typical dye release experiment with 0.306 μM melittin (c_M) and vesicles of 38 μM POPC (c_L). The original fluorescence signal F (arbitrary units) after the mixing is shown in the inset on the right-hand side. The average number of pores per vesicle, p (corrected to a uniform size of the vesicles) formed in the course of time (evaluated from F as pointed out in the text) is presented on the left. The solid curve was calculated according to Eqn. 8b employing the kinetic parameters $r_{po} = 3.5\cdot10^{-2}\ s^{-1}$, $r_{pi} = 2.75\cdot10^{-3}\ s^{-1}$, and $k = 4.25\cdot10^{-2}\ s^{-1}$. The dashed straight lines reflect the initial and intermediate rates (see text).

melittin and lipid concentrations. An example of original data is shown in the inset of Fig. 1. The measured fluorescence signal F apparently increases quite fast during the initial phase and then slows down substantially after about 1 min. It appears that the signal even comes to a virtual stop clearly below F_∞ at comparatively long times ($\gtrsim 30$ min) as was also observed by other authors with melittin [24] and similar agents [25,26]. In this report we shall confine ourselves to the time course within the first few minutes after having started the release experiment. By means of the Eqns. 7a,b the recorded F are converted to raw values of $p(t)$. These are corrected for spontaneous release of dye and in addition for the effect of vesicle size distribution (each acting in opposite direction). The former point was quantitatively examined in a series of appropriate control experiments without melittin. During the initial 90 s or so this interfering factor proved to be perfectly negligible. Afterwards we observed about 1% efflux within an additional period of 3 min. The inherent moderate degree of multidispersity of the vesicles has been taken into account by application of the procedure described previously [14]. This implies that the resulting p values refer to a defined uniform vesicle size. Appreciable corrections ($\gtrsim 10\%$ increase) are, however, applicable only at $p \gtrsim 1$. An example of the accordingly refined pore numbers per vesicle in the course of time is presented in Fig. 1.

As demonstrated by the slope of the typical $p(t)$ vs. t plot of Fig. 1 we generally observe that v_p decreases from an initial fast rate v_{po} to a substantially smaller intermediate value v_{pi}. This could be expressed by a single-exponential time function involving a time constant k according to

$$v_p = v_{pi} + (v_{po} - v_{pi})\, e^{-kt} \tag{8a}$$

so that application of Eqn. 6 leads to

$$p(t) = v_{pi} \cdot t + (v_{po} - v_{pi}) \cdot [(1 - e^{-kt})/k] \tag{8b}$$

With properly chosen values of v_{po}, v_{pi}, and k such a function can very well be fitted to our corrected p-data as displayed in Fig. 1. The initial slope is equal to v_{po} (reflected by the steep dashed line) while v_{pi} can be determined from the slope of the straight part of the curve which extrapolates to an intercept of $(v_{po} - v_{pi})/k$ on the ordinate axis.

In Fig. 2 we present some data of the initial rate v_{po} taken at variable melittin concentration, c_M, but constant lipid concentration, c_L (32 and 38 μM, respectively). As can be seen there is a rather well pronounced third power dependence. This suggests a possible third order rate law of v_{po} with respect to the lipid associated peptide concentration, r_l, when considering Eqn. 4. Since the partitioning equilibrium is

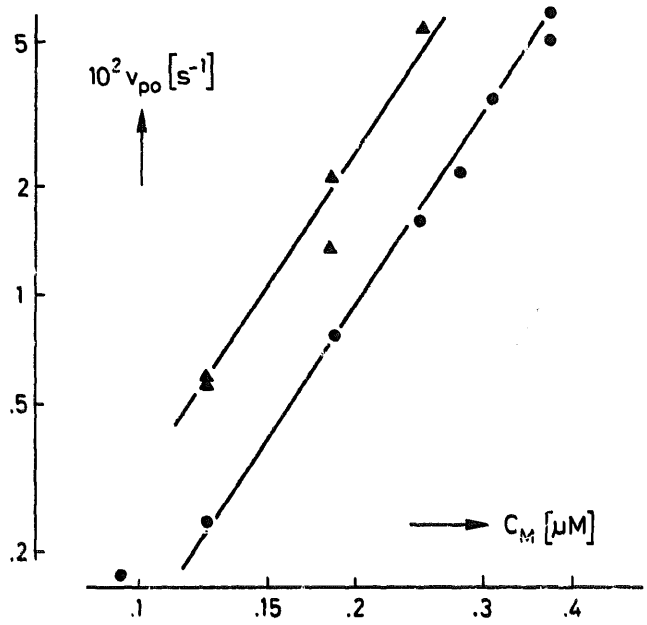

Fig. 2. Double-logarithmic plots of the initial rate of pore formation, v_{po} (in units of 10^{-2} pores per vesicle per second), as a function of the melittin concentration, c_M, at constant lipid (vesicle) concentration $c_L = 38$ μM (circles) and 32 μM (triangles), respectively. The straight lines have a slope of 3.

expected to be established comparatively fast (see above), c_M would be porportional to r_l provided α_l does not change. Actually the latter point is not rigorously satisfied but may be neglected in a first approximation (see the reconsideration given below).

We thus come to a putative rate law $v_{po} = k_p \cdot r_l^3$ (with a pertinent rate constant k_p) that is to be examined more closely. In particular, the effect of changing

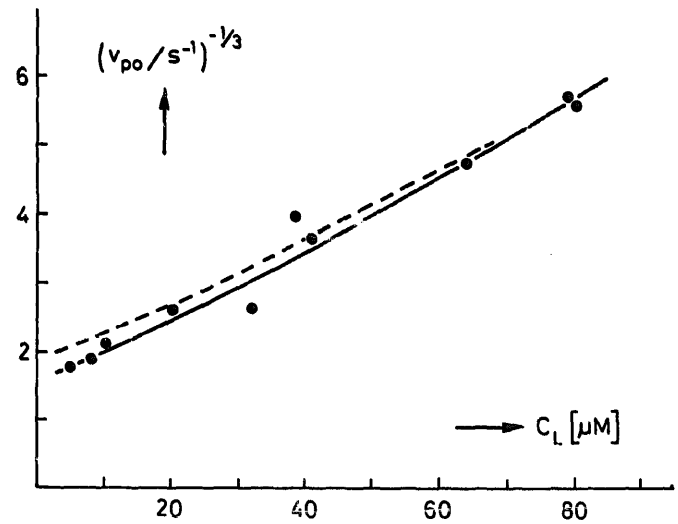

Fig. 3. Plot of $(1/v_{po})^{1/3}$ versus the lipid concentration at a constant melittin concentration of $c_M = 0.245$ μM. The solid curve (which is not a straight line) gives a best fit according to Eqn. 9 with $\Gamma_l = 7 \cdot 10^4$ M^{-1} and taking into account non-ideal peptide/lipid association described by a variable activity coefficient α_l. The dashed curve (shown for comparison) has been calculated with $\Gamma_l = 5 \cdot 10^4$ M^{-1}.

c_L at constant c_M will be of some quantitative significance. Because of Eqn. 4 we expect the data of Fig. 3 to be described by the relation

$$(1/v_{po})^{1/3} = B(\alpha_1 + \Gamma_1 c_L) \quad (9)$$

(B being a constant). In a first approximation α_1 may be taken as another constant so that a plot of $(1/v_{po})^{1/3}$ versus c_L would follow a straight line whose slope divided by the ordinate intercept results in Γ_1/α_1. Such a fit to the data is indeed possible yielding a quite reasonable value of $\Gamma_1/\alpha_1 \approx 3.4 \cdot 10^4$ M^{-1}. We prefer, however, to make proper allowance for a variable α_1 according to Eqn. 3. Under our conditions we have $b = 11.5$ and set $\nu_c = 1.85$ as determined previously for similar DOPC vesicles [15].

Then we find that $\Gamma_1 = 7 \cdot 10^4$ M^{-1} provides a very satisfactory best fit of Eqn. 9 to the data of Fig. 3. This value of Γ_1, on the other hand, is just of the order of magnitude determined for melittin interacting with other phosphatidylcholines, namely $\Gamma_1 = 3 \cdot 10^4$ M^{-1} in the case of DOPC [15] and $\Gamma_1 = 15 \cdot 10^4$ M^{-1} with DMPC (dimyristoylphosphatidilcholine) [16]. Just recently the authors of an independent study (with the same kind of POPC vesicles) reported $\nu_c = 1.9$ and $\Gamma_1 = 6(\pm 1) \cdot 10^4$ M^{-1} [27], in excellent agreement with our choice of these parameters. We have accordingly calculated for all our experimental sets of c_M, c_L the respective values of r_1 (by means of Eqn. 4) and then plotted all three kinetic parameters v_{po}, v_{pi}, and k as functions of r_1 (which varies from about $2 \cdot 10^{-3}$ up to $8 \cdot 10^{-3}$ with corresponding α_1 in the range of approx. 1.2 to 1.8). Double-logarithmic presentations are given in the Figs. 4 and 5. Within the scope of the inherent uncertainty of measurements v_{po} in fact conforms quite well to a third power dependence. In contrast, v_{pi} appears to follow a second-order rate law whereas k increases only in direct proportion to r_1.

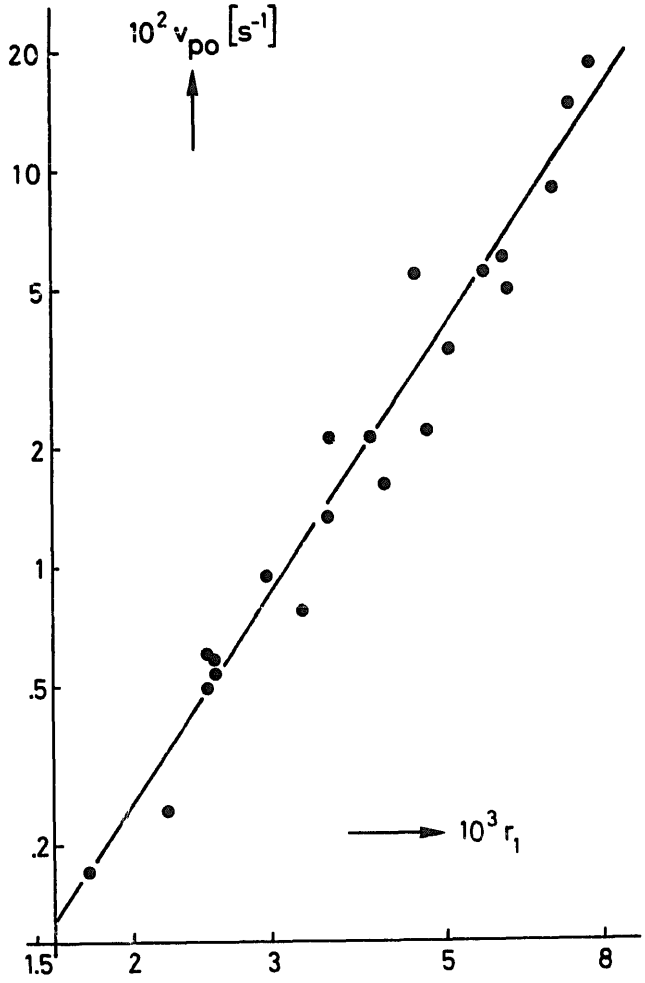

Fig. 4. Double-logarithmic plot of the initial pore formation rate as a function of the lipid associated melittin concentration r_1 (given on the abscissa in units of 10^{-3}, i.e., mmol peptid per mol lipid). The solid straight line has a slope of 3.

So far the rate v_p has been expressed in terms of pores per vesicle. For a more general discussion it appears appropriate to convert it into the number of pores per lipid. This calls for knowledge of the relevant geometric characteristics of the vesicles. The number of lipid molecules in the outer and the inner leaflets, respectively, can be derived as

$$\nu' = 4\pi(R+d)^2/A'_L, \quad \nu'' = 4\pi \cdot R^2/A''_L \quad (10a,b)$$

where A'_L and A''_L: areas per lipid molecule, R: inner vesicle radius, d: thickness of the bilayer. The trapped volume inside the vesicles then becomes

$$\bar{V}_i = (N_A A''_L/3) \cdot R/[1 + (A''_L/A'_L)/(1 + d/R)^2] \quad (11a)$$

As gathered from the literature [28] we have $A'_L = 74$ Å^2, $A''_L = 61$ Å^2, $d = 37$ Å. For $R \gtrsim 80$ Å this yields in good approximation

$$\bar{V}_i = 6.64 \cdot 10^{-3}(R - R_0) M^{-1}/\text{Å} \quad (R_0 = 30\,\text{Å}) \quad (11b)$$

We have measured $\bar{V}_i = 0.51(\pm 0.03)$ M^{-1} so that the average inner radius turns out to be equal to $R = 107(\pm 5)$ Å. This result agrees quite well with the linear average of R in a recent study of the vesicle size distribution by means of an electron microscope [14].

In our corrections of the original raw p-data the vesicle size distribution has been filtered out leading to plotted p which refer to a uniform vesicle size with an inner radius $R = 149$ Å [14]. In fact, the number of pores in a vesicle is expected to increase parallel to its membrane surface area (provided the rate per lipid is independent of the curvature). Larger vesicles then would contribute to v_p much more than in linear proportion to the radius. With the given R the corresponding number of lipid molecules per vesicle will be

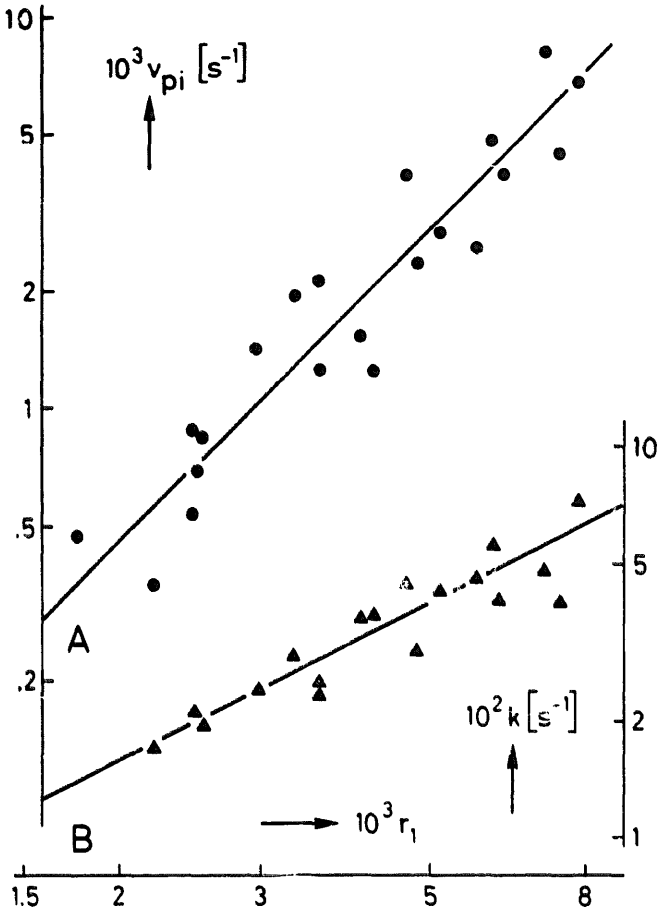

Fig. 5. Double-logarithmic plots of (A) the intermediate pore formation rate and (B) the time constant characterizing the slowing down of the rate versus the lipid associated melittin concentration. The solid straight lines have a slope of 2 and 1, respectively.

$\nu = 10600$ (a fraction $\beta = \nu'/\nu = 0.56$ making up the outer surface area). In order to convert pore numbers per vesicle into pore numbers per lipid we therefore simply divide p by this value of ν.

The results so far reported have been obtained under certain special conditions such as temperature, salt, pH, etc. as well as lipid composition and vesicle size. Naturally one should also investigate the effects of changes in these circumstances. Actually we can already present some relevant findings of interest from a number of preliminary experiments. On the one hand, it turned out that increasing the salt concentration (in steps of 0.1 M between 0.1 to 0.4 M NaCl) leads to a substantial speeding up of the pore formation. In another test we applied a transmembrane electric potential of around -100 mV (negative inside the vesicle) being established by adding valinomycin to an appropriate K^+ gradient. This resulted in a three times higher rate of channel activation than without such a potential (when no valinomycin was added) demonstrating that the underlying reaction pathway is definitely voltage-dependent. Finally we note some pertinent data observed with larger unilamellar vesicles having an approximate diameter of 100 nm (made by means of the extrusion technique). The number of pores formed per lipid there proved to fall much (i.e., by a factor of about 4) below the one measured with our small vesicles. Thus the inherent curvature of the bilayer membrane also appears to be a significant parameter of the relevant molecular mechanism.

Discussion

Naturally the melittin induced release of trapped marker must depend on the amount of peptide that is actually associated with the vesicle membrane. Under the present conditions practically only monomeric molecules exist in the aqueous [17,29] as well as lipid [15,30] environments, respectively. In addition, we have already presented evidence that the partitioning equilibrium is established in a time range substantially below one second. Since the overall release process takes much longer, we conclude that the pore formation rate should be a function of the equilibrium value of the ratio of associated melittin monomers per lipid. This proposition has in fact been verified by our above experimental results.

As pointed out in detail we have observed a transition from a third-order to a second-order dependence of r_p on r_1 in the course of time. Accordingly trimeric and dimeric aggregates of lipid associated melittin appear to play a significant role in the permeabilization process of the vesicle bilayer. This suggests that we deal with a formation of aggregates capable of functioning as water-filles pores in the membranes. They need not be particularly large. An inner diameter $\gtrsim 10$ Å would do (as estimated from the molecular weight of the dye). Melittin induced hemolytic pores in erythrocyte membranes naturally must be much larger (diameter $\gtrsim 55$ Å). Interestingly, the time course of hemolysis [10–12] looks quite similar to that of the marker release from lipid vesicles [24–26] including our present results. Such a resemblance, however, does not necessarily imply the same posssibly complex pathway, for instance a colloid osmotic mechanism. In hemolysis an initial melittin induced formation of smaller ion permeable pores may well lead to osmotically caused critical swelling of the cells and subsequent bursts as proposed [11]. Such a swelling of the vesicles under consideration here appears rather unlikely in view of the same salt concentration inside and outside.

We propose a simple kinetic mechanism of the pore formation being quantitatively consistent with all our present data. It implies aggregation steps starting from the monomeric state A_1 and eventually leading to the pore structure P (composed of a so far indefinite

number of monomers). This may be formulated by the scheme

$$2A_1 \underset{k_{21}}{\overset{k_{12}}{\rightleftharpoons}} A_2 \xrightarrow[A_1]{k_{23}} A_3 \xrightarrow[A_1]{} \cdots \xrightarrow[A_1]{} P \qquad (12)$$

where relevant rate constants are indicated. The aggregate states A_2, $A_3 \ldots P$ are meant to involve only negligible amounts of the lipid associated peptide. In addition, all aggregation steps beyond the dimer are assumed to be practically irreversible. In this scheme the amount of dimer per lipid, r_2, changes according to the rate equation

$$dr_2/dt = k_{12}r_1^2 - (k_{21} + k_{23}r_1)\cdot r_2 \qquad (13a)$$

Taking into account that the equilibrium value of r_1 is established comparatively fast and then remains practically constant, one readily obtains

$$r_2 = r_{2i} + (r_{20} - r_{2i})\, e^{-kt} \qquad (13b)$$

where $k = k_{21} + k_{23}r_1$ and r_2 changes from an initial value r_{20} to a steady-state level of $r_{2i} = (k_{12}/k)\cdot r_1^2$. Since the pore formation rate per lipid is equal to $dr_p/dt = dr_3/dt = k_{23}r_1r_2$, it immediately follows that

$$v_p = v_{pi} + (v_{po} - v_{pi})\, e^{-kt} \qquad (14)$$

with $v_{po} = \nu k_{23}r_1r_{20}$, $v_{pi} = \nu k_{23}r_1r_{2i}$. This is formally the same expression used to fit our data (see Eqn. 8a). In order to reconcile the observed dependences on r_1 with the present model mechanism we only have to put $k_{21} \ll k_{23}r_1$, $r_{20} = K_0r_1^2$. Then $v_{po} = \nu k_{23}K_0r_1^3$, $v_{pi} = \nu k_{12}r_1^2$, $k = k_{23}r_1$ involving the following numerical values $k_{23} = 8.0\ s^{-1}$, $k_{12} = 1.08\cdot 10^{-2}\ s^{-1}$ ($\nu = 10600$), $K_0 = 3.67$, and $k_{21} \ll 4\cdot 10^{-2}\ s^{-1}$.

Accordingly the measured rate of the melittin-induced pore formation is very well described by the proposed kinetic scheme 12. Dimerization of lipid associated peptide monomers will eventually become the rate-limiting step. One can readily verify that the dimers always comprise a negligible amount of the total peptide ($2r_2/r_1 \leqq 2K_0r_1 < 5\cdot 10^{-2}$). The same would apply to the higher aggregates including pore states. Thus r_1 is practically constant as determined by the fast monomer-monomer partitioning.

A peculiar point in the present rate model is the observed fast initial rate v_{po} exhibiting a third-order dependence on r_1 according to $r_{20} = K_0r_1^2$. It implies the occurrence of a rapidly formed dimer deposit that is gradually used up by the trimerization step. The origin of such a deposit, however, is not easily understandable. The appropriate rate must be very much faster than the one which can be expected from the above specified value of k_{12}. As a tentative explanation we envisage a fast change of the relevant physical properties of the bilayer structure being set off by the association of the peptide and resulting in a substantial drop of the dimer related rate constants within a time interval of about a second or less.

We must of course admit that the time scale of our experiments so far does not allow us to present the above model mechanism as a final one with regard to all its details. In order to resolve the individual reaction steps more conclusively the kinetic measurements must be extended to not only later times but particularly into the fast range well below a second. We have accordingly started pertinent work in this laboratory.

Acknowledgment

This work was supported by grant No. 31.25230.88 from the Swiss National Science Foundation.

References

1 Habermann, E. and Jentsch, J. (1967) Hoppe-Seyler Z. Physiol. Chem. 348, 37–50.
2 Dempsey, C.E. (1990) Biochim. Biophys. Acta 1031, 143–161.
3 Tosteson, M.T. and Tosteson, D.C. (1981) Biophys. J. 36, 109–116.
4 Tosteson, M.T. and Tosteson, D.C. (1984) Biophys. J. 45, 112–114.
5 Tosteson, M.T., Alvarez, O. and Tosteson, D.C. (1985) Regul. Pept. 8 (Suppl. 4), 39–45.
6 Tosteson, M.T., Levy, J.J., Caporale, L.H., Rosenblatt, M. and Tosteson, D.C. (1987) Biochemistry 26, 6627–6631.
7 Kempf, Ch., Klausner, R.D., Weinstein, J.N., Renswoude, J.V., Pincus, M. and Blumenthal, R. (1982) J. Biol. Chem. 257, 2469–2476.
8 Hanke, W., Methfessel, Ch., Wilmsen, H.-U., Katz, E., Jung, G. and Boheim, G. (1983) Biochim. Biophys. Acta 727, 108–114.
9 Pawlak, M., Stankowski, S. and Schwarz, G. (1991) Biochim. Biophys. Acta 1062, 94–102.
10 DeGrado, W.F., Musso, G.F., Lieber, M., Kaiser, E.T. and Kézdy, F.J. (1982) Biophys. J. 37, 329–338.
11 Tosteson, M.T., Holmes, S.J., Razin, M. and Tosteson, D.C. (1985) J. Membrane Biol. 87, 35–44.
12 Portlock, S.H., Clague, M.J. and Cherry, R.J. (1990) Biochim. Biophys. Acta 1030, 1–10.
13 Weinstein, J.N., Yoshikami, S., Henkart, P., Blumenthal, R. and Hagins, W.A. (1977) Science 195, 489–492.
14 Schwarz, G. and Robert, C.H. (1990) Biophys. J. 58, 577–583.
15 Schwarz, G. and Beschiaschvili, G. (1989) Biochim. Biophys. Acta 979, 82–90.
16 Stankowski, S. and Schwarz, G. (1990) Biochim. Biophys. Acta 1025, 164–172.
17 Quay, S.C. and Condie, C.C. (1983) Biochemistry 22, 695–70018.
18 Shipolini, R.A., Gallewaert, G.L., Cottrell, R.C., Doonan, S., Vernon, C.A. and Banks, B.E.C. (1971) Eur. J. Biochem. 20, 459–468.
19 Huang, C. (1969) Biochemistry 8, 344–351.
20 Ames, B.N. and Dubin, D.T. (1960) J. Biol. Chem. 235, 769–775.
21 Böttcher, C.J.F., Van Gent, C.M. and Fries, C. (1961) Anal. Chim. Acta 24, 203–204.
22 Roseman, M.A., Lentz, B.R., Sears, B., Gibbes, D. and Thompson, T.E. (1978) Chem. Phys. Lipids 21, 205–222.
23 Weinstein, J.N., Klausner, R.D., Innerarity, T., Ralston, E. and Blumenthal, R. (1981) Biochim. Biophys. Acta 647, 270–284.
24 Portlock, S.H., Clague, M.J. and Cherry, R.J. (1990) Biochim. Biophys. Acta 1030, 1–10.

25 Matsuzaki, K., Harada, M., Hanada, T., Funakoshi, S., Fujii, N., Yajima, H. and Miyajima, K. (1989) Biochim. Biophys. Acta 981, 130–134.
26 Menestrina, G., Forti, S. and Gambale, F. (1989) Biophys. J. 55, 393–405.
27 Beschiaschvili, G. and Baeuerle, H.D. (1991) Biochim. Biophys. Acta 1068, 195–200.
28 Huang, C. and Mason, J.T. (1978) Proc. Natl. Acad. Sci. USA 75, 308–310.
29 Schwarz, G. and Beschiaschvili, G. (1988) Biochemistry 27, 7826–7831.
30 Altenbach, Ch. and Hubbell, W.L. (1988) Proteins Struct. Funct. Genet. 3, 230–242.